

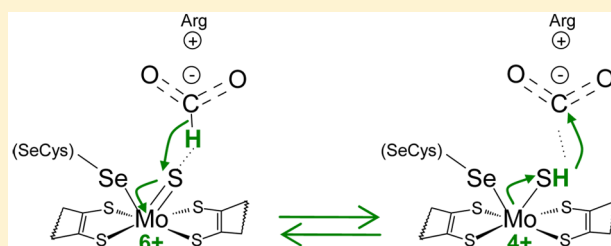
Reduction of Carbon Dioxide by a Molybdenum-Containing Formate Dehydrogenase: A Kinetic and Mechanistic Study

Luisa B. Maia,* Luis Fonseca, Isabel Moura, and José J. G. Moura*

UCIBIO, REQUIMTE, Departamento de Química, Faculdade de Ciências e Tecnologia, Universidade Nova de Lisboa, 2829-516 Caparica, Portugal

S Supporting Information

ABSTRACT: Carbon dioxide accumulation is a major concern for the ecosystems, but its abundance and low cost make it an interesting source for the production of chemical feedstocks and fuels. However, the thermodynamic and kinetic stability of the carbon dioxide molecule makes its activation a challenging task. Studying the chemistry used by nature to functionalize carbon dioxide should be helpful for the development of new efficient (bio)catalysts for atmospheric carbon dioxide utilization. In this work, the ability of *Desulfovibrio desulfuricans* formate dehydrogenase (Dd FDH) to reduce carbon dioxide was kinetically and mechanistically characterized. The Dd FDH is suggested to be purified in an inactive form that has to be activated through a reduction-dependent mechanism. A kinetic model of a hysteretic enzyme is proposed to interpret and predict the progress curves of the Dd FDH-catalyzed reactions (initial lag phase and subsequent faster phase). Once activated, Dd FDH is able to efficiently catalyze, not only the formate oxidation (k_{cat} of 543 s^{-1} , K_m of $57.1 \text{ }\mu\text{M}$), but also the carbon dioxide reduction (k_{cat} of 46.6 s^{-1} , K_m of $15.7 \text{ }\mu\text{M}$), in an overall reaction that is thermodynamically and kinetically reversible. Noteworthy, both Dd FDH-catalyzed formate oxidation and carbon dioxide reduction are completely inactivated by cyanide. Current FDH reaction mechanistic proposals are discussed and a different mechanism is here suggested: formate oxidation and carbon dioxide reduction are proposed to proceed through hydride transfer and the sulfo group of the oxidized and reduced molybdenum center, $\text{Mo}^{6+}=\text{S}$ and $\text{Mo}^{4+}\text{-SH}$, are suggested to be the direct hydride acceptor and donor, respectively.



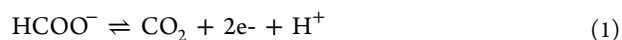
1. INTRODUCTION

The global energy demand and the present high dependence on fossil fuels have caused the increase in the atmospheric carbon dioxide concentration for the highest values since records began.¹ Due to its significant green-house effect, carbon dioxide rise is responsible for large and unpredictable impacts on the world climate, besides being responsible for ocean warming and acidification (ocean is the major sink of carbon dioxide).² Conversely, the carbon dioxide abundance and low cost make it an interesting source for the production of useful synthetic value-added chemicals and fuels^{1,3}—in an “imitation” of the ancient carbon dioxide fixation into the reduced organic compounds that originated the fossil fuels used nowadays. As a result, there is a huge interest in the development of strategies to scavenge atmospheric carbon dioxide and to efficiently produce reduced carbon compounds suitable to be subsequently used as fuels or chemical feedstocks.

A major challenge has been the thermodynamic and kinetic stability of the carbon dioxide molecule that makes its laboratory/industrial activation a very difficult task. However, nature has developed several pathways for carbon dioxide fixation, using different enzymes and mechanistic/chemical strategies to cleave the C–O bond (reduction to carbon monoxide) and form C–C (e.g., addition to ribulose 1,5-bisphosphate) and C–H bonds (reduction to formate).^{3d,4}

Understanding the mechanistic/chemical strategies employed by those diverse enzymes would certainly contribute to the development of new efficient (bio)catalysts for the atmospheric carbon dioxide utilization.^{1,3d,5} In this work, we focused on the carbon dioxide reduction to formate catalyzed by the formate dehydrogenase (FDH) from the sulfate-reducing bacteria *Desulfovibrio desulfuricans* (Dd FDH). The interest in formate arises from formate being thought as a viable energy source (easier to store and transport than hydrogen) and as a stable methanol or methane source.

FDH enzymes catalyze the reversible two-electron oxidation of formate to carbon dioxide (eq 1). These enzymes are involved in a multiplicity of pathways, from the biosynthetic metabolism to the energy metabolism, where they participate in fermentation and respiratory chain pathways.⁶ As a result, FDHs are a group of heterogeneous proteins, harboring diverse redox centers or no redox centers at all, and displaying different subunit compositions and quaternary structures.



FDHs can be divided into two major classes, based on their metal-content. One class comprises NAD-dependent enzymes,

Received: April 17, 2016

Published: June 27, 2016

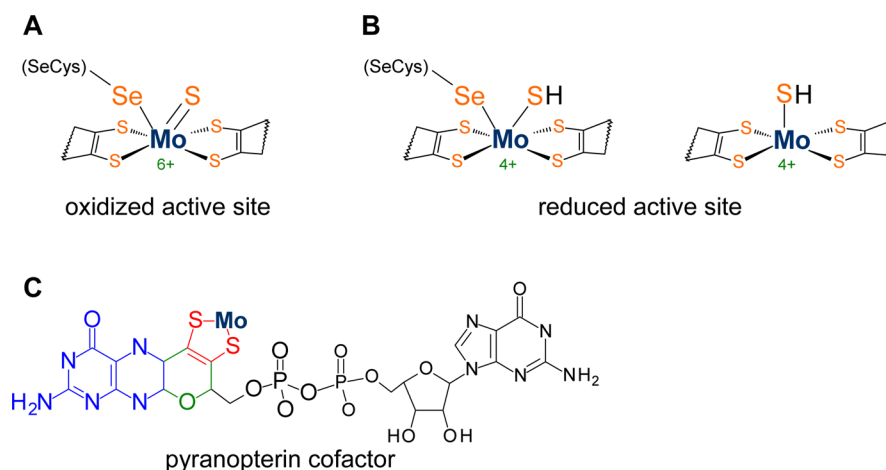


Figure 1. Structures proposed for the active site of *Desulfovibrio desulfuricans* FDH. (A) Structure that is consensually accepted for the oxidized state of the catalytic center of Dd FDH and other metal-dependent FDH enzymes. (B) Structure for the reduced state of the catalytic center suggested by the results of Boyington et al.¹⁰ and Jormakka et al.¹² (left) and by the results of Raaijmakers and Romão¹¹ (right). The complete structure of pyranopterin cofactor is presented in panel (C); in panels (A) and (B), for simplicity, only the dithiolene moiety of the pyranopterin cofactor is represented. The pyranopterin cofactor molecule is formed by pyrano(green)-pterin(blue)-dithiolene(red)-methylphosphate(black) moieties; in FDHs, the cofactor is found esterified with a guanosine monophosphate (black). The dithiolene (—S—C=C—S—) group forms a five-membered ene-1,2-dithiolene chelate ring with the molybdenum atom (or with the tungsten atom, in the case of W-FDHs).

belonging to the *D*-specific dehydrogenases of 2-oxoacids family, that have no metal ions or other redox cofactors; this is the class of metal-independent FDHs.⁷ These enzymes are widespread, being found in bacteria, yeasts, fungi and plants. The other class comprises the metal-dependent FDHs and it includes only prokaryotic enzymes that hold different redox centers and whose active sites harbor one molybdenum or one tungsten atom that mediates the formate oxidation.⁶ Accordingly, metal-containing FDHs can be subdivided as molybdenum-containing FDH (Mo-FDH) and tungsten-containing FDH (W-FDH).

Sulfate-reducing bacteria of the *Desulfovibrio* genus contain diverse Mo-FDHs and W-FDHs⁸ that are interesting systems for mechanistic studies aiming to develop new efficient (bio)catalysts for carbon dioxide utilization. The periplasmatic FDH from *D. desulfuricans* (Dd FDH) is a heterotrimeric ($\alpha\beta\gamma$; ≈ 135 kDa) molybdenum-containing enzyme, harboring four *c* hemes, two [4Fe-4S] centers and one molybdenum center.^{8c,i} The molybdenum center is the active site, where formate is oxidized, while the other six redox centers are thought to be involved in the subsequent intramolecular electron transfer to the physiological acceptor. Although the tridimensional structure of the Dd FDH is not known, the molybdenum center is suggested to hold one molybdenum atom coordinated by the four sulfur atoms of two pyranopterin guanosine dinucleotide cofactor molecules (Figure 1C), as is characteristic of this enzyme family, the molybdenum/tungsten-*bis* pyranopterin guanosine dinucleotide (Mo/W-*bis* PGD)-containing enzyme family.^{6c,9} By analogy with other FDHs whose tridimensional structure is known (*Escherichia coli* Mo-FDH H^{10,11} and Mo-FDH N¹² and *D. gigas* W-FDH^{8f} (Figure S1 in Supporting Information)), the molybdenum coordination sphere of the Dd FDH in the oxidized resting state is suggested to be completed by a conserved essential selenocysteine residue (Mo—Se(Cys)) and a sulfo terminal group (Mo=S), in a distorted trigonal prismatic coordination geometry (Figure 1A)^{8c,i} The active site pocket is thought to be comprised of a conserved arginine and a histidine residue, which were suggested to play a role in catalysis (Figure S1).^{10,11}

In this work, we showed for the first time that the Dd Mo-FDH is able to catalyze, not only the formate oxidation, but also the carbon dioxide reduction to formate. We established that the reaction is thermodynamically and kinetically reversible and demonstrated that the carbon dioxide reduction occurs at relatively high rates ($k_{\text{cat}}^{\text{app}}$ of 46.6 s^{-1}) and with a high affinity ($K_{\text{m}}^{\text{app}}$ of $15.7 \mu\text{M}$) for carbon dioxide. A comprehensive kinetic model is suggested to interpret and predict the FDH kinetic properties. We have been quite involved in understanding the FDH-catalyzed reaction mechanism and the results described herein led us to rethink our previous mechanistic proposal for FDHs and to support a different chemical strategy for both carbon dioxide reduction and formate oxidation.

2. MATERIALS AND METHODS

2.1. Enzyme Purification. *D. desulfuricans* ATCC 27774 cells were grown in lactate-nitrate medium, under anaerobic conditions, at 37 °C, and collected by centrifugation at the end of the exponential phase, as previously described.⁸ⁱ Dd FDH was purified as previously described, with all the purification steps performed aerobically, at 4 °C.⁸ⁱ Protein concentration was determined by the Lowry method. Routine formate oxidation activity assays were carried out under anaerobic conditions, following the benzyl viologen reduction at 555 nm ($\epsilon = 12000 \text{ M}^{-1} \text{ cm}^{-1}$), as previously described.⁸ⁱ FDH was incubated with 130 mM β -mercaptoethanol, in 60 mM Tris-HCl, pH 7.6, for 10 min, after which, 10 mM sodium formate was added and allowed to incubate for further 10 min; the reaction was, then, initiated by the addition of 7.5 mM benzyl viologen.

2.2. Kinetic Characterizations. All kinetic assays were carried out under anaerobic conditions (argon atmosphere), at 22 °C. All solutions were made with “carbon dioxide-free water”: fresh distilled and deionized water was boiled vigorously for 15 min and allowed to cool under argon atmosphere, in sealed flasks (the fresh water solubility of carbon dioxide is 3.5 times lower at 100 °C than at 22 °C (0.47 versus 1.6 gCO₂/L water, 1 atm)); this procedure enabled us to obtain a water with a much lower carbon dioxide concentration. The buffer used was 100 mM triethanolamine pH 8.0 and 7.0, for formate oxidation assays and carbon dioxide reduction assays, respectively. To improve the assays reproducibility (and eliminate a highly hazardous volatile compound), the β -mercaptoethanol used

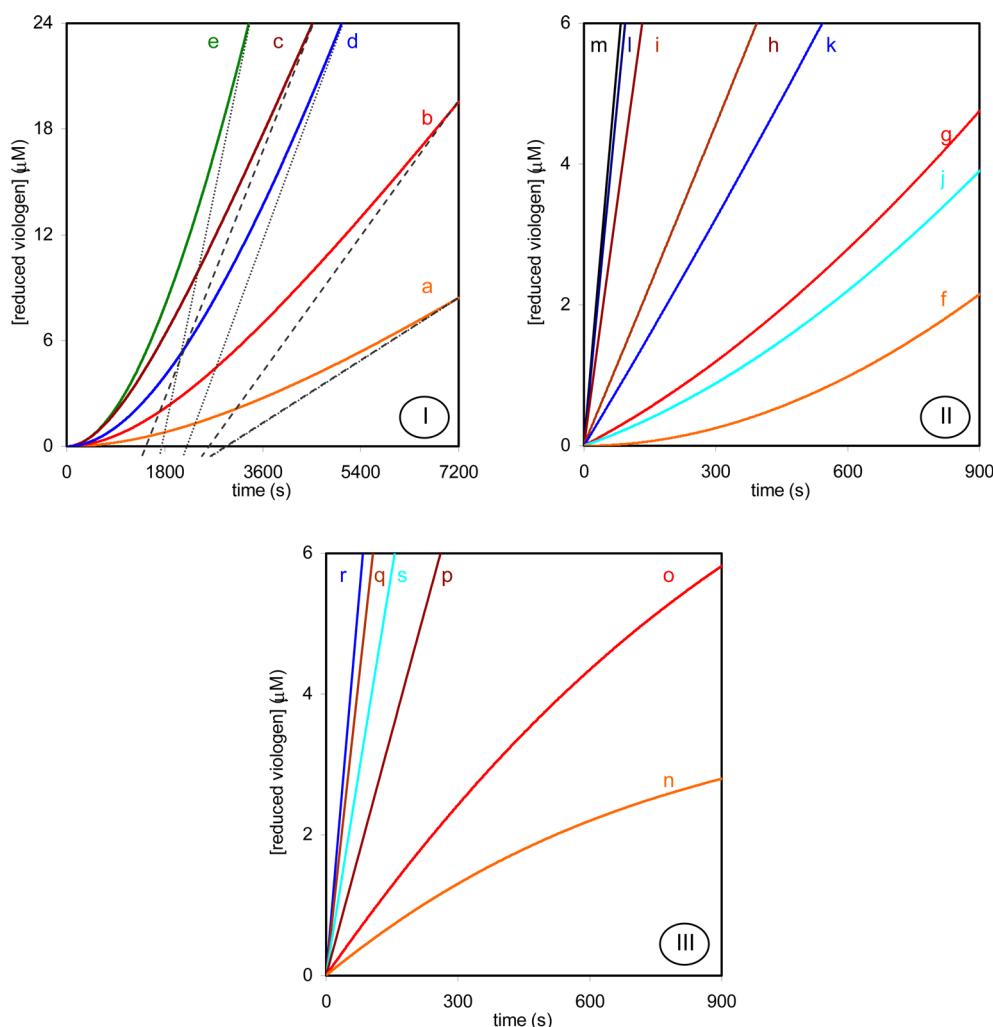
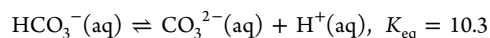
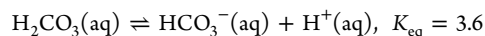
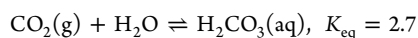


Figure 2. Representative time courses of Dd FDH-catalyzed formate oxidation. Panel I: (a) 100 μM formate and 0.01 nM FDH, (b) 250 μM formate and 0.01 nM FDH, (c) 1000 μM formate and 0.01 nM FDH, (d) 100 μM formate and 0.05 nM FDH, (e) 100 μM formate and 0.1 nM FDH. The gray dashed line aims to highlight how different the lag phase extents are. The reactions were monitored following the benzyl viologen reduction, as described under section 2.2.; all reagents were added immediately before the beginning of the assay (with no previous incubations) and the reactions were initiated by the addition of 5 mM oxidized viologen. Panel II: In one set of assays (orange, red, dark red and brown lines), 100 μM formate and 0.1 nM FDH were previously incubated for zero (f), 10 min (g), 20 min (h) and 30 min (i); after the indicated time period, the reactions were initiated by the addition of 5 mM oxidized viologen. In another set of assays (turquoise, blue and dark blue lines), 2.5 μM reduced viologen and 0.1 nM FDH were previously incubated for zero (j), 5 min (k) 10 min (l) and 30 min (m); after the indicated time period, the reactions were initiated by the addition of 100 μM formate plus 5 mM oxidized viologen. The reactions were followed through the benzyl viologen reduction (section 2.2.); in the second set of assays, the initial concentration value of reduced viologen was subtracted to allow the direct comparison with the results of the first set. Panel III: In one set of assays (orange, red, dark red and brown lines), 0.1 nM FDH and 2.5 μM reduced viologen were previously incubated for 10 min; the reactions were, then, initiated by the addition of 100 μM formate plus 50 μM (n), 100 μM (o), 1 mM (p) or 5 mM (q) oxidized viologen. In another set of assays (light blue and blue lines), 0.1 nM FDH and 10 μM (r) or 50 μM (s) reduced viologen were previously incubated for 10 min; the reactions were, then, initiated by the addition of 100 μM formate plus 5 mM oxidized viologen. The reactions were followed through the benzyl viologen reduction (section 2.2.); the initial concentration value of reduced viologen was subtracted to allow the direct comparison of the results.

during routine assays (section 2.1.) was here replaced by 0.5 mM dithiothreitol. Reduced viologen (benzyl or methyl) was obtained by reduction with zinc pellets; its reduction was followed spectrophotometrically at 555 nm (benzyl viologen; $\epsilon = 12000 \text{ M}^{-1} \text{ cm}^{-1}$) or 605 nm (methyl viologen; $\epsilon = 11300 \text{ M}^{-1} \text{ cm}^{-1}$). Sodium carbonate was used as the source of carbon dioxide. The carbon dioxide concentrations indicated in this work were calculated using the following equilibrium constants; in accordance, at pH 7.0, the concentration of carbon dioxide is 0.166 of the total carbonated species present.



Diverse kinetic assays were performed, with the reagents (prepared as described above) being added in different orders and without or with previous incubations for various time periods. Appropriate controls were carried in each case, to account for the nonenzymatic viologen reduction/oxidation. The individual conditions of each assay are described in the figures captions and text; each “condition” was reproducibly repeated a minimum of three times. The steady-state apparent kinetic parameters were estimated by the Hanes method¹³

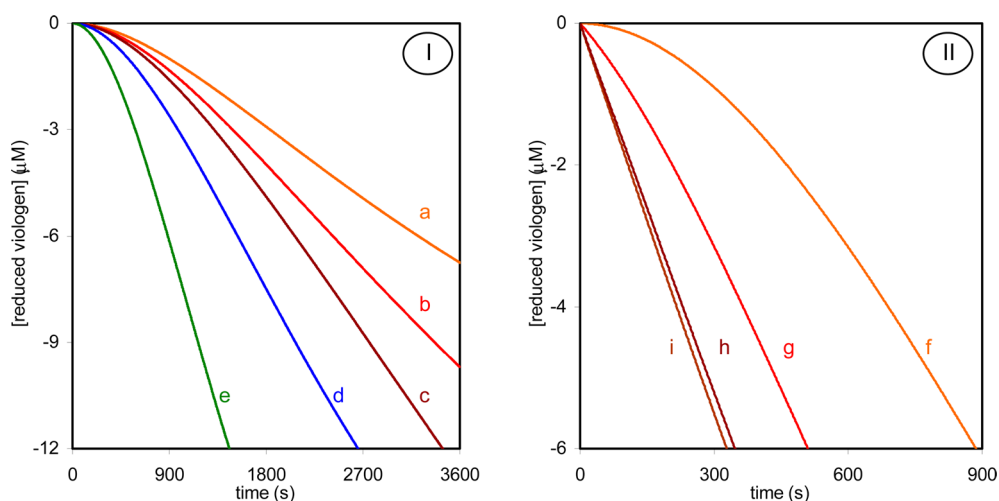


Figure 3. Representative time courses of Dd FDH-catalyzed carbon dioxide reduction. Panel I: (a) 20 μM carbon dioxide and 0.05 nM FDH, (b) 50 μM carbon dioxide and 0.05 nM FDH, (c) 200 μM carbon dioxide and 0.05 nM FDH, (d) 50 μM carbon dioxide and 0.1 nM FDH, (e) 50 μM carbon dioxide and 0.25 nM FDH. The reactions were monitored following the oxidation of reduced viologen, as described under section 2.2.; all reagents were added immediately before the beginning of the assay (with no previous incubations) and the reactions were initiated by the addition of 200 μM reduced viologen. Panel II: 0.25 nM FDH and 200 μM reduced viologen were previously incubated for zero (f), 5 min (g) 10 min (h) and 30 min (i); after the indicated time period, the reactions were initiated by the addition of 50 μM carbon dioxide. In both panels, the initial reduced viologen concentration was set to zero and the y axis values are expressed as negative values that reflect the consumption (oxidation) of reduced viologen.

from the initial rates determined at least in triplicate. The rate equations were derived with the King–Altman method.¹³

3. RESULTS AND DISCUSSION

3.1. Transients during FDH-Catalyzed Formate Oxidation (Initial Lag Phases). The kinetic studies of FDH-catalyzed formate oxidation rely on following spectrophotometrically the reduction of an artificial electron acceptor, usually methyl or benzyl viologen: while formate is oxidized to carbon dioxide by oxidized FDH, the viologen should be stoichiometrically reduced by the reduced FDH. However, the observed viologen absorbance changes are very complex, with the reaction time courses displaying an initial lag phase that is followed by the expected steady-state, faster, viologen reduction phase only after some minutes (Figure 2). This kinetic behavior is not exclusive to the Dd FDH and initial lag phases were also described with, e.g., *Syntrophobacter fumaroxidans* W-FDH1.¹⁴

The lag phase extent was found to be dependent on the enzyme and formate concentrations, with shorter lag phases being obtained with higher enzyme or formate concentrations (Figure 2, curves a–e). Moreover, the lag phase extent can be shortened, or eliminated, if the FDH is incubated with formate, before the addition of viologen: no previous incubation leads to the longest lag phase (Figure 2, curve f); FDH incubation with formate for zero to <30 min leads to time courses with progressively shorter lag phases (Figure 2, curves g and h, for 10 and 20 min incubation); FDH incubation with formate for 30 min eliminates the lag phase (Figure 2, curve i). On the contrary, the previous enzyme incubation with oxidized viologen (from 1 to 60 min), with formate being added only in the end, does not diminish or abolish the initial lag phase. We named this process of eliminating the initial lag phase as “formate activation”.

Once the FDH surpasses the lag phase and becomes kinetically active, the catalytic cycle proceeds with high rates of formate oxidation. Under this regime, in the presence of a high (20 mM) formate concentration, the catalysis is not disturbed

even if the anaerobic conditions are abolished by opening the spectrophotometric cell and allowing the atmospheric dioxygen and carbon dioxide to diffuse into the reaction mixture. This “resistance” toward the presence of dioxygen attests the robustness of this enzymatic system and is a value-added to its potential use as a catalyst for carbon dioxide utilization.

The necessity of a substrate to activate an enzyme is not the only phenomenon that can originate transients. To identify other possible mechanisms of FDH activation, we searched for other ways to decrease/eliminate the initial lag phases. We found that the initial lag phase can be decreased by the addition of reduced viologen: if FDH and formate are mixed together immediately before the beginning of the assay (with no previous incubations) and the reaction is initiated by the addition of oxidized plus reduced viologen (and not of only oxidized viologen), the initial lag phase is considerably decreased, as can be observed by comparing curves f (adding only oxidized viologen) and j (adding oxidized plus reduced viologen), in Figure 2. Moreover, the previous FDH incubation with reduced viologen, before the addition of formate, shortens, or eliminates, the initial lag phase: no previous incubation leads to a determined lag phase (Figure 2, curve j); FDH incubation with reduced viologen for 5 min leads to a shorter lag phase (Figure 2, curve k); FDH incubation with reduced viologen for 10 or 30 min eliminates the lag phase (Figure 2, curves l and m). In summary, FDH incubation with reduced viologen is able to increase the initial rate of formate oxidation, eliminating the initial lag phase, as the incubation with substrate formate does. By analogy, we named this activation process as “reduced viologen activation”. However, it should be emphasized that the time of incubation needed to visually abolish the lag phase is considerably shorter in the “reduced viologen activation” than in the “formate activation” process (compare curves l (10 min) and i (30 min incubation), in Figure 2).

The effect of reduced viologen on the initial rate of formate oxidation could be taken as suggesting that formate reacts only with reduced FDH and not with oxidized FDH. If this was the

case, then the role of reduced viologen in the activation process would be to reduce FDH for the enzyme to be able to react with formate. However, this is not the case, because the initial rate of formate oxidation increases with increasing concentrations of oxidized viologen (Figure 2, curves n–q), regardless of the concentration of reduced viologen molecules present (Figure 2, curves q–s). Another experimental evidence that formate does not react with reduced FDH comes from the observation that both activation processes (“formate activation” and “reduced viologen activation”) lead to similar initial rates of viologen reduction (Figure 2, curves i and l or m), showing that the initial presence of reduced FDH does not lead to a higher rate of reaction. As a result, we concluded that formate reacts only with oxidized FDH, as would be expected for an oxidation reaction.

3.2. Transients during FDH-Catalyzed Carbon Dioxide Reduction (Initial Lag Phases). The kinetic studies of FDH-catalyzed carbon dioxide reduction rely on following spectrophotometrically the oxidation of viologen: while carbon dioxide is reduced to formate by reduced FDH, the reduced viologen should be stoichiometrically oxidized by the oxidized FDH.

In this work, using a carbonate solution as the source of carbon dioxide, we demonstrated for the first time that the Mo-FDH from *Desulfovibrio desulfuricans* is able to catalyze, not only the formate oxidation, but also the carbon dioxide reduction. Yet, the time course curves of carbon dioxide reduction were found to be also complex, with an initial lag phase followed by a faster, steady-state phase only after a few minutes (Figure 3), as observed in the formate oxidation curves. The lag phase extent was found to be dependent on the enzyme and reduced viologen concentrations, with shorter lag phases being obtained with higher concentrations (Figure 3, curves a–e). As can be anticipated, the previous FDH incubation with reduced viologen (with the reaction being initiated by the addition of carbon dioxide) shortens, or eliminates, the initial lag phase (Figure 3, curves f–i): no previous incubation leads to the longest lag phase (Figure 3, curve f); FDH incubation with reduced viologen for 5 min leads to a time course with a shorter lag phase (Figure 3, curve g); FDH incubation with formate for more than 10 min eliminates the lag phase (Figure 3, curve h and i for 10 and 30 min incubation). Of note, the time of incubation needed to obtain the maximal initial rate of carbon dioxide reduction is similar to the time needed to obtain the maximal initial rate of formate oxidation when the “reduced viologen activation” is used (compare curve l in Figure 2 with curve h in Figure 3). Therefore, reduced viologen is able to increase the initial rate of both formate oxidation and carbon dioxide reduction, eliminating the initial lag phase, in a way that is kinetically similar in both reactions.

We could not find the experimental conditions under which carbon dioxide could decrease/eliminate the initial lag phase (through a process that would be parallel to the “formate activation” by formate) or any other experimental conditions that lead to a decrease in/elimination of the initial lag phase.

In summary, Dd FDH is able to catalyze both the formate oxidation and carbon dioxide reduction, but it has to be first activated to display high catalytic activities. Using the “reduced viologen activation” process, both reactions display similar kinetics of activation.

3.3. Kinetic Model for the FDH-Catalyzed Formate Oxidation and Carbon Dioxide Reduction. To interpret

the complete time course curves of FDH (initial lag phase and subsequent faster phase) and the two activation processes, we propose the kinetic model of hysteresis described in Figure 4.¹³

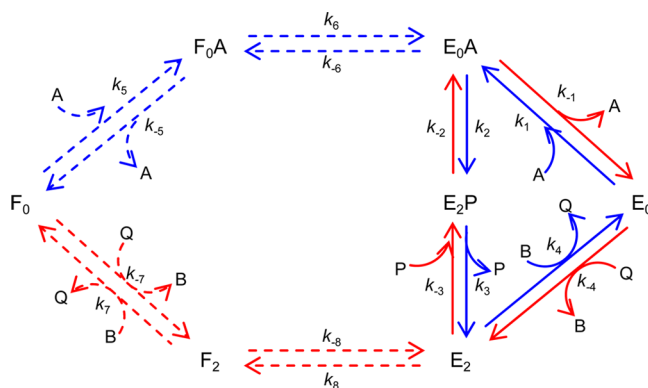


Figure 4. Integrated kinetic model for the formate oxidation (blue lines) and carbon dioxide reduction (red lines) catalyzed by Dd FDH. The detailed description of the model can be found in [Supporting Information](#). Dashed lines represent activation steps, “formate activation” in blue and “reduced viologen activation” in red. F and E represent two FDH forms, whose details are explained in text; the subscripts “0” and “2” denote oxidized and reduced molybdenum center. A, B, P and Q represent formate, oxidized viologen, carbon dioxide and reduced viologen, respectively. Although the viologen (B) is an one-electron reducer/oxidant, include two consecutive steps for enzyme reduction or oxidation ($E_0 \rightleftharpoons E_1 \rightleftharpoons E_2$) would only complicate the model, without providing any extra useful information; thus, for simplicity, viologen was considered as a two-electron reducer/oxidant and k_4/k_{-4} and k_7/k_{-7} are thought as “global rate constants” that describe the two steps of one-electron reduction/oxidation. Another simplification was introduced when the FDH was allowed to have only two oxidation states, oxidized (F_0/E_0) and reduced (F_2/E_2). Although the Dd FDH enzyme can be reduced with as much as 8 electrons (because it harbors, besides the molybdenum center, four c hemes and two iron/sulfur centers), consideration of all the possible oxidation states would only complicate the model, without providing any extra useful information. Moreover, during catalysis, under steady-state, it is expected that the enzyme “recycles” between only two oxidation states, “n” and “n + 2”, as was shown for other enzymes acting on two-electrons reducible/oxidizable substrates. Accordingly, k_5/k_{-5} plus k_6/k_{-6} and k_7/k_{-7} plus k_8/k_{-8} are thought as “global rate constants” that describe the activation processes of inactive FDH molecules that have their molybdenum center oxidized and the other redox centers in all the thermodynamically possible combinations of oxidation states. In addition, because FDHs are a group of heterogeneous enzymes, displaying different redox centers and subunit compositions, this approach also allows this model to be applied to other FDH enzymes.

In parallel to what was suggested earlier by Mota et al.,¹⁵ we propose that FDH exists in two forms, here denominated F and E. The *as purified* FDH exists in a thermodynamically stable, but kinetically inactive F form.¹⁶ In order to oxidize formate or reduce carbon dioxide, the enzyme F form has to be converted into the kinetically active, but thermodynamically much less favorable species E. The direct F into E conversion is suggested to be unfavorable and can not account for the formation of the E form. Instead, it is suggested that the formation of the E form is dependent on the interaction of the oxidized F form (F_0) with formate (A), through the steps controlled by k_5 and k_6 (blue dashed lines), or on the interaction of F_0 with reduced viologen (Q), through the steps controlled by k_{-7} and k_{-8} (red dashed lines).

Under these conditions, the time course curve of formate oxidation will display an initial lag phase if the conversion of F into E is considerably slower than the main catalytic steps, k_1 , k_2 , k_3 , k_4 (blue lines) (the detailed description of the model can be found in [Supporting Information](#)). This effect is illustrated by the simulated time course curves (w) to (z) in [Figure S2](#), where it is shown the effect of the k_6 magnitude on the length of the lag phase. The dependence of the lag phase extent on the formate and FDH concentrations observed experimentally ([Figure 2](#)) is modeled through the step controlled by k_5 , which is dependent on F_0 and formate concentrations. The longer lag phases observed with the “formate activation”, comparatively to the “reduced viologen activation” process, is modeled assuming that the k_5 plus k_6 steps are slower than the k_{-7} plus k_{-8} steps. The following faster phase of the time course arises when, after some catalytic cycles, the kinetically active E form builds up and continues the catalysis through the faster $k_1 \rightarrow k_2 \rightarrow k_3 \rightarrow k_4$ cycle, circumventing the slow conversion of F into E.

Regarding the carbon dioxide reduction reaction, since its “reduced viologen activation” is kinetically similar to the one observed during formate oxidation, we followed the same reasoning and suggest that the FDH-catalyzed carbon dioxide reduction follows the kinetic model depicted in the red lines of [Figure 4](#). Therefore, in parallel to what was described above, the time course curve of carbon dioxide reduction will display an initial lag phase, if the conversion of F into E is considerably slower than the main catalytic steps, k_{-4} , k_{-3} , k_{-2} , k_{-1} . The following faster phase arises when the kinetically active E form builds up and is able to continue the catalysis through the faster $k_{-4} \rightarrow k_{-3} \rightarrow k_{-2} \rightarrow k_{-1}$ cycle, circumventing the slow conversion of F into E.

Hence, the kinetic model here proposed, without making any assumption about the structure of the F and E forms, or about the conversion process, is able to interpret the sigmoidal time courses displayed by FDH, providing a description of the kinetics of the “formate activation” and “reduced viologen activation” processes.¹⁷

Regarding the actual physical/chemical changes responsible for the enzyme activation process, it was in this work shown that, while oxidized viologen or carbon dioxide do not exert any effect, reduced viologen, as well as formate, facilitate the activation. Therefore, we concluded that the activation is not dependent on the specific interaction between formate and the active site, because that specific interaction is not present in the “reduced viologen activation” process and because carbon dioxide is not able to activate the enzyme. Carbon dioxide is a substrate of Dd FDH (as demonstrated here) and of other FDHs^{6d,6e,8k,14,18} and has the same chemical structure, with two oxygen atoms, as formate (albeit with no net charge); so, if the FDH activation was dependent on the specific interaction of substrate with the active site, carbon dioxide should also be able to promote the enzyme activation.

Alternatively, we suggest that the FDH activation is dependent on the reduction of the enzyme, which can be achieved with formate, viologen or other artificial reducer: we suggest that the reduction of the enzyme, or the reduction of one key redox center of the enzyme (recall that Dd FDH holds six redox centers, besides the molybdenum center), would trigger a conformational change that facilitates the substrate (formate and carbon dioxide) binding and/or its catalysis. Moreover, we suggest that the “formate activation” is slower than the “reduced viologen activation” process, because the inactive FDH form would not promote the efficient formate

binding/oxidation; consequently, the enzyme reduction by formate is slower than its reduction by a nonspecific reducer and the enzyme activation is, thus, also slower. Carbon dioxide or oxidized viologen are not able to activate the FDH, because they can not reduce the enzyme.

The rationalization of the reductive activation process at the molecular/atomic level is, however, particularly challenging with the present knowledge of FDHs. Nonetheless, some hypotheses for the FDH reductive activation are envisaged and discussed in [Supporting Information](#). Other enzymes of the Mo/W-*bis* PGD enzyme family were described to also need a reductive activation (including nitrate reductases from *R. sphaeroides*,^{19a,20a} *E. coli*,^{20b} *Paracoccus pantotrophus*^{20c} and dimethyl sulfoxide reductase from *R. sphaeroides*^{19b,20d}), which suggests that the reductive activation could be a common phenomenon to this enzyme family.

3.4. Steady-State Kinetic Characterization of the FDH-Catalyzed Formate Oxidation and Carbon Dioxide Reduction. Although the kinetic model here proposed is described by a complex rate equation (eq S1, in [Supporting Information](#)), it predicts that the formate oxidation and carbon dioxide reduction would follow saturation kinetics in the absence of initial carbon dioxide and formate (respectively) and presence of a constant viologen concentration (as eq S1 can be simplified, under that conditions, to the classic Michaelis–Menten equation with apparent kinetic parameters, as described in eqs S2 and S3, respectively). As expected, the formate oxidation reaction was found to follow saturation kinetics, with an $k_{\text{cat}}^{\text{app}}$ of 543 s⁻¹ and an $K_{\text{m}}^{\text{app}}$ of 57.1 μM ([Figure S3](#)), values that are in agreement with the ones previously reported by Mota et al.¹⁵ ($k_{\text{cat}}^{\text{app}}$ of 347 s⁻¹ and $K_{\text{m}}^{\text{app}}$ of 64 μM). The carbon dioxide reduction reaction was also found to follow saturation kinetics, with an $k_{\text{cat}}^{\text{app}}$ of 46.6 s⁻¹ and an $K_{\text{m}}^{\text{app}}$ of 15.7 μM ([Figure S4](#)).

Several FDHs were described to be able to catalyze the carbon dioxide reduction under appropriate conditions.^{6d,6e,8k,14,18} Yet, the great majority of FDHs display carbon dioxide reduction rates lower^{14,18c,e,gi} or around 1 s⁻¹,^{18b,j-1} with considerably higher rates of formate reduction. In this scenario, the Dd FDH stands out as a strikingly fast and efficient carbon dioxide reducer. In spite of the formate oxidation being ≈10 times faster, the Dd FDH specificity for carbon dioxide ($k_{\text{app,CO}_2} = k_{\text{cat,app,CO}_2}/K_{\text{m,app,CO}_2} = 2.97 \mu\text{M}^{-1} \text{s}^{-1}$) is only ≈3 times lower than for formate ($k_{\text{app,HCOO}^-} = 9.51 \mu\text{M}^{-1} \text{s}^{-1}$), what favors the reduction of carbon dioxide when formate is present in lower concentrations.

3.5. Reversible Interconversion of Carbon Dioxide and Formate. Formate oxidation is a thermodynamically reversible reaction (eq 1). The FDH-catalyzed formate oxidation would also be a thermodynamically reversible reaction if the FDH molybdenum center can be poised at the appropriate reduction potentials, to generate Mo⁶⁺ or Mo⁴⁺, in order to make the formate oxidation or carbon dioxide reduction (respectively) thermodynamically possible. The above results, showing that the enzyme can catalyze both the formate oxidation and the carbon dioxide reduction, demonstrate that the Dd FDH molybdenum center can be poised at those adequate reduction potentials and, thus, that the Dd FDH-catalyzed reaction is thermodynamically reversible. Those results also demonstrate that both reactions, when run separately, are kinetically feasible (that is, FDH catalyzes the carbon dioxide reduction in the absence of initial formate and

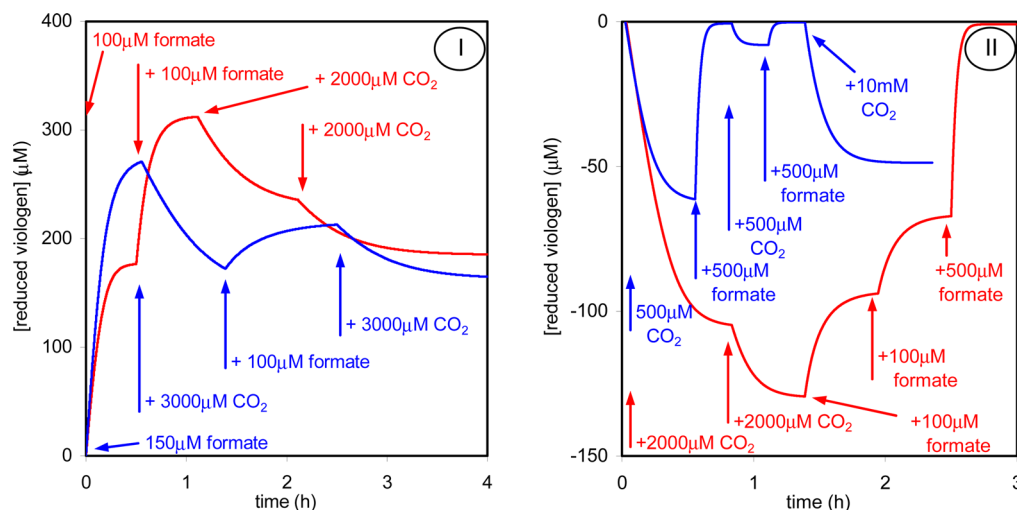


Figure 5. Representative time courses of Dd FDH-catalyzed formate oxidation and carbon dioxide reduction. Panel I, Formate oxidation system. Red line: The oxidation of 100 μM formate by 0.5 nM FDH was followed for 30 min, until the equilibrium was approximately attained. 100 μM formate was then added and the system evolved to oxidize the additional formate, with the simultaneous reduced viologen increase. After a second equilibrium position was approximately attained, 2000 μM carbon dioxide was added and the system now evolved to consume that carbon dioxide, resulting in a decrease in the reduced viologen concentration. A second addition of carbon dioxide (2000 μM) leads to a further decrease in the reduced viologen. Blue line: In a similar assay, the reduced viologen concentration was decreased/increased/decreased to respond to the addition of carbon dioxide/formate/carbon dioxide after an initial approximate equilibrium of formate oxidation had been attained. Panel II, Carbon dioxide reduction system. Red line: The reduction 2000 μM carbon dioxide by 1 nM FDH was followed for 50 min, until the equilibrium was approximately attained. 2000 μM carbon dioxide was then added and the system evolved to reduce the additional carbon dioxide, with the simultaneous decrease in reduced viologen concentration. After a second equilibrium position was approximately attained, 100 μM formate was added and the system evolved to consume that formate, resulting in an increase in the reduced viologen. A second (100 μM) and a third (500 μM) addition of formate restored the reduced viologen. Blue line: In a similar assay, the reduced viologen concentration was decreased/increased/decreased/increased/decreased to respond to the addition of carbon dioxide/formate/carbon dioxide/formate/carbon dioxide. The initial reduced viologen concentration was set to zero and the y axis values are expressed as negative values that reflect the consumption (oxidation) of reduced viologen.

presence of reduced viologen and FDH catalyzes the formate oxidation in the absence of initial carbon dioxide and presence of oxidized viologen). Hence, it remains to be shown that, even in the presence of formate, FDH can catalyze the carbon dioxide reduction (and vice versa).

In order to prove this, we undertook a series of assays, starting with the reaction of formate oxidation and adding, subsequently, carbon dioxide (Figure 5, Panel I), or starting with the reaction of carbon dioxide reduction and adding, subsequently, formate (Figure 5, Panel II). In all cases, the reaction followed the direction expected to consume the substrate added latter, leading to a new equilibrium position. These results demonstrate that, regardless the presence of formate plus carbon dioxide and reduced plus oxidized viologen, FDH can “switch” between formate oxidation/carbon dioxide reduction to respond to an external change on the concentration of formate or carbon dioxide, “choosing” the reaction that would favor the equilibrium (eq 1). In other words, these results demonstrate that the Dd FDH-catalyzed reaction is, in fact, thermodynamically and kinetically reversible.

3.6. Inhibition by Cyanide. Cyanide was previously identified as a mixed-inhibitor of the Dd FDH-catalyzed formate oxidation, characterized by a competitive and uncompetitive inhibition constants of 420 and 1634 μM , respectively (assays carried out by adding cyanide to the reaction mixture of the activity assay).⁸¹ However, our experience with the mammalian molybdoenzymes xanthine oxidase (XO) and aldehyde oxidase (AO) made us think that cyanide could react with FDH in a more dramatic way. The XO and AO active site harbors a terminal sulfo group coordinated to the molybdenum atom ($\text{Mo}=\text{S}$),^{6c,9} as the FDH enzymes

hold (at least those FDHs whose crystal structure is known; Figure S1). This sulfur atom, in XO and AO, can be removed by incubation with cyanide, to yield a catalytically inactive desulfo-form that harbors a $\text{Mo}=\text{O}$ instead of the $\text{Mo}=\text{S}$ group.²¹

A similar inactivation process could occur in Dd FDH, but the active site sulfo group in the *as purified* Dd FDH does not seem to be accessible to react with the cyanide molecule. We overcame this constraint by promoting the FDH activation before its incubation with cyanide: (i) Dd FDH was incubated with an equimolar concentration of formate, for 30 min, and then oxidized with viologen; (ii) subsequently, FDH was incubated overnight with 10 mM cyanide; (iii) cyanide/thiocyanide were, then, removed by gel filtration (on a small Sephadex G-25 column). The resulting FDH sample displayed no formate oxidation or carbon dioxide reduction activity (this procedure was repeated four times and none of the four FDH samples obtained in this way displayed activity). Control assays were performed, where FDH was treated in exactly the same way, but in the absence of cyanide. By the end of the control assay, the FDH samples retained $82 \pm 8\%$ of the initial activity (mean \pm standard deviation from three independent assays), demonstrating that the FDH inactivation is, in fact, due to the action of cyanide. Hence, we concluded that cyanide is able to completely inactivate Dd FDH, most likely by removing the sulfo group of the active site, as is well documented and consensually recognized to occur in XO and AO.^{6c,9,21} The procedure necessary to obtain the cyanide-inactivated FDH further corroborates that Dd FDH is purified in a kinetically inactive form that has to be activated to display high catalytic activity or to be completely inactivated by cyanide.

The cyanide ability to completely inactivate Dd FDH and FDHs from other sources (*Methanobacterium formicicum*,^{22a} *Alcaligenes eutrophus*^{22b} or *E. coli*^{22c}), suggests that the active site sulfo group should play a critical role in the FDH catalysis. This group is consensually recognized as the hydride acceptor in the oxidized molybdenum center ($\text{Mo}^{6+}=\text{S}$) of XO and AO^{6c,9,21,23} and of other enzymes of the xanthine oxidase family,^{6c,9b} as well as, the hydride donor in the reduced center ($\text{Mo}^{4+}\text{-SH}$) of hydroxybenzoyl-CoA reductase.²⁴ Hence, we suggest that the sulfo group should play a similar role in the FDH catalysis, with the oxidized $\text{Mo}^{6+}=\text{S}$ and reduced $\text{Mo}^{4+}\text{-SH}$ acting as hydride acceptor and donor in formate oxidation and carbon dioxide reduction, respectively.

4. A NEW LOOK AT THE REACTION MECHANISM OF FDH

Mo-FDH or W-FDH-catalyzed formate oxidation occurs at the molybdenum or tungsten center of the enzymes.⁶ This reaction does not involve oxygen atom transfer: the product of formate oxidation is carbon dioxide and not hydrogen carbonate (eq 2),²⁵ as was clearly demonstrated by the formation of $^{13}\text{C}^{16}\text{O}_2$ gas during the oxidation of ^{13}C -labeled formate in ^{18}O -enriched water.²⁶ Therefore, to oxidize formate, FDH has to abstract one proton plus two electrons (eq 1) or one hydride (eq 3) from the formate molecule.



(The FDH reaction mechanism is believed to be similar in Mo-FDHs and W-FDHs and in enzymes harboring and active site selenocysteine or cysteine residue,²⁷ but, for simplicity and improve readability, henceforth, only a selenocysteine-containing Mo-FDH will be mentioned.)

To explain the FDH reaction, a few mechanistic hypotheses were put forward in the past decade, based on the structural data described by Raaijmakers and Romão¹¹ for the *E. coli* FDH H (Figure S1.C).^{11,15,29–31} In particular, extended DFT calculations carried out by our group and collaborators launched the comprehensive “sulfur shift mechanism”.^{15,30} This mechanistic proposal involves (i) the active site selenocysteine dissociation from the molybdenum atom (to create a vacant coordination position for formate binding), (ii) the necessary direct binding of formate to the molybdenum atom ($\text{Mo}-\text{OCO}(\text{H})$) and (iii) the formate $\text{C}\alpha$ proton abstraction by the selenium atom of the dissociated selenocysteine residue (Figure S5; the detailed description of this mechanism can also be found in Supporting Information).

However, a careful reanalysis of our published experimental data on FDHs and the new results described in this work (and by others) forced us to reassess our previous mechanistic proposal. There are three key aspects for which the sulfur shift mechanism can not, presently, provide a satisfactory explanation. (i) FDH activation: A sulfur shift triggered specifically by the formate molecule can not explain the “reduced viologen activation” process or the inability of carbon dioxide to promote the activation of FDH, as discussed in section 3.3. (ii) FDH-substrate complex: The sulfur shift mechanism suggests the formation of a reduced molybdenum-formate complex ($\text{Mo}^{4+}\text{-OCO}(\text{H})$). This suggestion can not be easily reconciled with our present kinetic results that demonstrate that the rate of formate oxidation is dependent on the oxidized

enzyme concentration and that formate reacts only with oxidized FDH (as would be expected for an oxidation reaction; section 3.1.). Conversely, the rate of carbon dioxide reduction is dependent on the reduced enzyme concentration (as would be expected for a reduction reaction; section 3.2.). Furthermore, as far as we know, presently, there is no unambiguous experimental evidence that formate (or carbon dioxide) binds directly to the FDH molybdenum atom, nor there is experimental consensus regarding the selenocysteine dissociation from the FDH molybdenum atom in the reduced state (these two aspects are discussed in Supporting Information). (iii) FDH reaction: The sulfur shift mechanism does not dictate any catalytic role for the molybdenum sulfo group ($\text{Mo}=\text{S}$). However, the complete FDH inactivation by cyanide suggests that the sulfo group should play a critical role in the catalysis of both formate oxidation and carbon dioxide reduction, as discussed in section 3.6. In addition, the new mechanistic hypotheses must describe the ability of FDH to catalyze both the formate oxidation and the carbon dioxide reduction, in a global, thermodynamically and kinetically, reversible reaction (sections 3.4., 3.5.).

These aspects led us to presently support a different chemical strategy for the FDH-catalyzed formate oxidation and carbon dioxide reduction, widening the recent mechanistic hypothesis of Niks et al. for the *R. eutropha* FDH-catalyzed formate oxidation.³² In this novel proposal, the focus is shifted from the selenocysteine and turned into the sulfo group of the active site, with the formate oxidation/carbon dioxide reduction occurring via hydride transfer (eq 3, not eq 1) and with the molybdenum sulfo group acting as the direct hydride acceptor/donor, respectively, as described below.

4.1. The Molybdenum Sulfo Group Is the Direct Hydride Acceptor/Donor. As discussed in section 3.6., we support³² that the active site sulfo group should play a central role in the FDH catalysis, with the oxidized $\text{Mo}^{6+}=\text{S}$ and reduced $\text{Mo}^{4+}\text{-SH}$ acting as hydride acceptor and donor in formate oxidation and carbon dioxide reduction, respectively. The highly covalent terminal sulfur atom of the sulfo group, with an available S π -bond, is well suited to accept a hydride and, thus, facilitate the cleavage of a C–H bond. Moreover, the $\text{p}K_{\text{a}}$ values of the molybdenum coordinated ligands allow this “twin” behavior of hydride acceptor/donor:³³ the $\text{p}K_{\text{a}}$ values change dramatically with the oxidation state of the metal and determine that the higher oxidation states should hold deprotonated ligands ($\text{Mo}^{6+}=\text{S}$, suitable to accept a hydride), while the lower oxidation states should hold protonated ligands ($\text{Mo}^{4+}\text{-SH}$, suitable to donate a hydride).

The proposed role for the sulfo group is in complete agreement with our previous EPR spectroscopic studies with Dd FDH⁸¹ that showed that the formate $\text{C}\alpha$ hydrogen atom is transferred to an acceptor group located within magnetic contact to the molybdenum atom (studies described in Supporting Information). The presence of a strongly coupled formate-derived hydrogen within magnetic contact to the molybdenum atom was also described in the 1990s in the *E. coli* FDH H²⁶ and, more recently, in the *R. eutropha* FDH.³² These EPR data, obtained with different FDHs, shows that, if the selenocysteine is dissociated from the molybdenum during catalysis, it is not the hydrogen atom acceptor (because the residue would be far from the molybdenum magnetic influence); if the selenocysteine remains bound during catalysis, it would not be able to accept the hydrogen atom.³⁴ In both

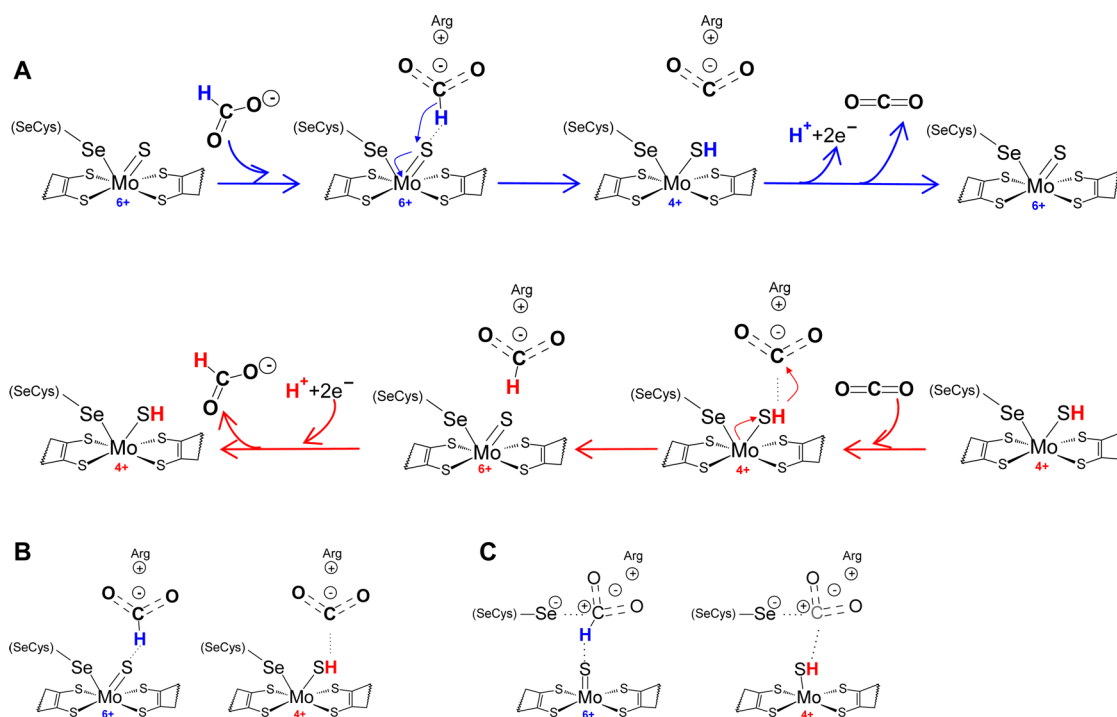


Figure 6. Reaction mechanism proposed for the FDH-catalyzed formate oxidation and carbon dioxide reduction. (A) Formate oxidation (blue arrows) and carbon dioxide reduction (red arrows). The two reactions were represented separately to be easier to follow the individual steps in each case, but the blue and red arrows represent one unique reversible reaction, that can be driven in both directions, depending on the prevalent molybdenum oxidation/reduction state and on the presence of formate/carbon dioxide. (B) and (C) represent hypothetical substrate binding modes to a hexa-coordinated and penta-coordinated molybdenum center.

cases, the only molybdenum ligand that can accept the formate α hydrogen is the sulfo group.

4.2. Formate Oxidation and Carbon Dioxide Reduction Occur via Hydride Transfer. Following the role proposed for the sulfo group, the formate oxidation should occur through hydride transfer (eq 3) and not via one proton plus two electrons transfer (eq 1), as had been suggested so far. In fact, the abstraction of one hydride from the formate molecule should be more facile than the abstraction of one proton, because, in the first case, the direct reaction product is the final, stable carbon dioxide molecule, while, in the second case, is a carbanion, $(\text{CO}_2)^{2-}$, whose formation is dependent on a very high $\text{p}K_{\text{a}}$ value ($\text{p}K_{\text{a}1} = 3.75$ and $\text{p}K_{\text{a}2} > 14$). Further evidence that formate is intrinsically a good hydride donor comes from the metal-independent NAD-dependent FDHs that employ a surprisingly simple chemistry to carry out catalysis:⁷ the enzyme binds formate and NAD^+ in close proximity of each other (1.4 Å distance between H-(formate) and C4-(pyridine ring)) and forces NAD^+ to acquire a bipolar conformation, which increases the NAD^+ electrophilicity and, thus, facilitates the hydride transfer. The reaction, then, proceeds by straightforward hydride transfer from formate to NAD^+ . The reverse addition of hydride to carbon dioxide to produce formate finds further support in several synthetic transition metal-hydride complexes that mimic the FDH catalysis.³⁵

4.3. Reaction Mechanism. According to the above reasoning, the FDH-catalyzed formate oxidation is suggested to occur as described by the blue arrows in Figure 6.A. Formate oxidation is initiated by formate binding to the oxidized active site, but not directly to the molybdenum atom. Following the example provided by the metal-independent FDH, whose

formate binding site harbors an arginine and asparagine residues,⁷ we suggest that the conserved arginine, and possibly histidine, of Mo/W-FDHs would be essential to drive the α hydrogen of formate toward the sulfo ligand, by establishing hydrogen bond(s) with its oxygen atom(s). Moreover, we suggest that azide (N_3^-), that is isoelectronic with carbon dioxide, binds tightly to the same site as formate and not directly to the molybdenum atom, as our previous EPR studies had already suggested.^{8i,36} The binding of azide and formate to the same site explains why azide is a powerful inhibitor of both metal-independent^{7c} and metal-dependent FDHs.^{8i,26} A similar reasoning would apply to the inhibitor nitrite (isoelectronic with formate).

Formate oxidation, then, proceeds by straightforward hydride transfer from formate to the sulfo group of the oxidized molybdenum center, $\text{Mo}^{6+}=\text{S}$, leading to the formation of $\text{Mo}^{4+}\text{-SH}$ and carbon dioxide. This chemical strategy—*direct hydride transfer*—was also recently suggested by Niks et al.³² to explain the *R. eutropha* FDH-catalyzed formate oxidation. The catalytic cycle is closed with the oxidation of Mo^{4+} to Mo^{6+} , via intramolecular electron transfer to other(s) redox center(s), and carbon dioxide being eventually released. The $\text{p}K_{\text{a}}$ of the sulfo ligand of the now oxidized Mo^{6+} favors its deprotonation³³ and the initial oxidized active site center, $\text{Mo}^{6+}=\text{S}$, is regenerated. Under noncatalytic conditions, as the ones created in EPR experiments, the molybdenum one-electron oxidation should be favored, leading to the formation of the EPR detectable $\text{Mo}^{5+}\text{-SH}$ species (as was described in Supporting Information).

The carbon dioxide reduction is suggested to follow the reverse reaction mechanism (Figure 6.A, red arrows). Carbon dioxide binds to the reduced active site, holding a protonated

sulfo group, $\text{Mo}^{4+}\text{-SH}$ (as its $\text{p}K_{\text{a}}$ determines³³), but not directly to the molybdenum atom. We suggest that it would bind to the same site as formate (and azide), with the conserved arginine, and possibly histidine, anchoring its oxygen atom(s) through hydrogen bond(s) and orienting its carbon atom toward the protonated sulfo ligand. In an approximated way, based on the inhibition and Michaelis–Menten constants, we suggest that the “binding strength” to the Dd FDH would follow the order carbon dioxide ($K_{\text{m}} \approx 15.7 \mu\text{M}$) > azide ($K_{\text{i}} \approx 33 \mu\text{M}$ ⁸¹) > formate ($K_{\text{m}} \approx 57.1 \mu\text{M}$). Carbon dioxide reduction proceeds through straightforward hydride transfer from the protonated sulfo group of the reduced molybdenum center, $\text{Mo}^{4+}\text{-SH}$, to the carbon atom of carbon dioxide, whose LUMO have predominant C-*p* orbital character. This yields a formate moiety and $\text{Mo}^{6+}=\text{S}$. The catalytic cycle is closed with the reduction of Mo^{6+} to Mo^{4+} , via intramolecular electron transfer from other(s) redox center(s), and formate being eventually released. The now reduced Mo^{4+} favors the sulfo group protonation³³ and the initial reduced active site center, $\text{Mo}^{4+}\text{-SH}$, is regenerated. Overall, the balance between formate oxidation versus carbon dioxide reduction would be determined by the availability of formate versus carbon dioxide and by the ability to produce Mo^{6+} versus Mo^{4+} centers, with the oxidation state of the center determining the protonation state of the sulfo group (hydride affinity) in an “automatic” way.

The active site selenocysteine (or cysteine²⁷) residue remains bound to the molybdenum atom throughout the entire catalytic cycle of both formate oxidation and carbon dioxide reduction (Figure 6). A permanent hexa-coordination sphere (Figure 6.B) should hinder the oxygen (or sulfur) atom transfer activity that is characteristic of the molybdenum/tungsten-containing enzymes^{6c,9} and, thus, allow the FDH to act exclusively as a hydrogen atom transfer enzyme. The same reasoning applies to the benzoyl-CoA reductase that catalyzes the transfer of two hydrogen atoms to the benzene ring and whose tungsten center was described to be permanently hexa-coordinated.^{37,38} A sulfur/selenium rich coordination may also be necessary to increase the covalency of the Mo–S bond of the sulfo group and/or to modulate the metal reduction potential. However, the presence of a selenocysteine selenium (more covalent) or of a cysteine sulfur (less covalent) should alter the reaction energetic profile. It is, thus, reasonable that the cysteine-containing enzymes compensate the absence of a selenium atom by introducing small changes in the active site (as described for other proteins that contain either selenium or sulfur, e.g.,⁴⁰ recall that all tridimensional structures known are from selenocysteine-containing FDHs).

Nevertheless, the present lack of experimental consensus regarding the selenocysteine (or cysteine) positioning in the active site—*unbound or bound to the molybdenum atom*—led us to think also about the scenario of a dissociated selenocysteine residue. The direct hydride transfer to/from the sulfo group itself does not seem to require that the selenocysteine remains bound to the molybdenum atom. It can be envisaged a dissociated selenocysteine involved in anchoring the substrate molecule in the active site, as was suggested in the 1990s by Heider and Bock,⁴¹ and activating the *C α* (Figure 6.C). A similar role is found, e.g., in the NAD-dependent aldehyde dehydrogenases, in which the aldehyde molecule is bound to an active site cysteine residue via a $-(\text{Cys})\text{S}\cdots\text{CO}(\text{R})(\text{H})$ bond. A dissociated selenocysteine residue could also be involved in the proton releasing pathway, from the sulfo group to the exterior of the active site, even though the chalcogens tendency to form

hydrogen bridges ($\text{O} > \text{S} > \text{Se}$) might question this suggestion. Certainly, future experimental work (crystallographic and spectroscopic) is needed to understand the structural ambiguities of FDH; high resolution structures are needed to confirm the existence of the two alleged conformations of the selenocysteine (cysteine)-containing polypeptide loop and to discuss the catalytic relevance of each conformation.

Overall, the mechanistic strategy here presented is inclusive and could be followed by both Mo-FDHs and W-FDHs, as well as by enzymes harboring an active site selenocysteine or cysteine residue. Moreover, this hydride transfer mechanism allows the identification of an “universal” chemical strategy for all FDHs, metal-independent and metal-dependent enzymes: formate binding in a close proximity to an oxidized, electrophilic, hydride acceptor and carbon dioxide binding in a close proximity of a reduced hydride donor. How this is achieved at the atomic level is obviously different in metal-independent and metal-dependent enzymes: while the first ones use a NAD^+ or a NADH molecule, the metal-dependent enzymes use a $\text{Mo}^{6+}=\text{S}$ or a $\text{Mo}^{4+}\text{-SH}$ center (respectively for formate oxidation and carbon dioxide reduction).⁴² Most important, the hydride transfer mechanism presents an elegant and straightforward way to make the FDH reaction energetically feasible in both directions (reversible): the oxidation state of the molybdenum center “automatically” defines the presence of an “oxidized center plus hydride acceptor” or of a “reduced center plus hydride donor”, thus guaranteeing the formation of the right “redox/hydride partner” for the formate oxidation or carbon dioxide reduction.

New theoretical calculations are being performed, considering the molybdenum coordination spheres here suggested for the oxidized and reduced FDH active site. As far as we know, the hydride transfer to/from an oxidized $\text{Mo}^{6+}=\text{S}$ /reduced $\text{Mo}^{4+}\text{-SH}$ had not been yet modeled, nor was considered the reaction as reversible. From an energetic point of view, it can be anticipated that the hydride transfer mechanism avoids the endothermic step of the Se–S cleavage (to yield $-(\text{Cys})\text{Se}$ plus S-Mo ; Figure S5 (iii)) and has the additional advantage of producing carbon dioxide or formate in only one step.

5. CONCLUSION

The Dd FDH is suggested to be purified in an inactive form that has to be activated, through a “formate activation” or “reduced viologen activation” process, to display high catalytic rates or be inactivated by cyanide. A kinetic model of hysteresis is described (Figure 4) to provide a framework to interpret the initial lag phase and the following faster phase of the FDH time course curves. Once activated, Dd FDH is able to efficiently catalyze, not only the formate oxidation ($k_{\text{cat}}^{\text{app}}$ of 543 s^{-1} , $K_{\text{m}}^{\text{app}}$ of $57.1 \mu\text{M}$), but also the carbon dioxide reduction ($k_{\text{cat}}^{\text{app}}$ of 46.6 s^{-1} , $K_{\text{m}}^{\text{app}}$ of $15.7 \mu\text{M}$), in an overall reaction that is thermodynamically and kinetically reversible.

The reaction mechanism of FDH was revisited and, integrating *old* and new experimental results, we suggest that both formate oxidation and carbon dioxide reduction proceed through hydride transfer and that the sulfo group of the oxidized and reduced molybdenum center, $\text{Mo}^{6+}=\text{S}$ and $\text{Mo}^{4+}\text{-SH}$, are the direct hydride acceptor and donor, respectively (Figure 6).

Besides the fundamental biochemical and biological interest, Dd FDH is of potential biotechnological interest for carbon dioxide transformation and/or formate production. Comparatively to other FDHs, the majority of which displays very low

rates of carbon dioxide reduction, the Dd FDH is a strikingly fast and efficient carbon dioxide reducer, with a high $k_{\text{cat}}^{\text{app}}$ value of $\approx 50 \text{ s}^{-1}$ and a specificity for carbon dioxide that is only ≈ 3 times lower than the specificity for formate, what favors the reduction of carbon dioxide when formate is present in lower concentrations ($K_{\text{m}}^{\text{app,CO}_2} = 15.7 \mu\text{M}$, $K_{\text{m}}^{\text{app,HCOO}^-} = 57.1 \mu\text{M}$). Most important, once the enzyme is activated and the catalysis is proceeding at high rates, the FDH reaction is “resistant” to the presence of dioxygen. Overall, the kinetic features of Dd FDH place it in a good position to be considered as of potential biotechnological interest and the kinetic and mechanistic data presented in this work aim to contribute to inspire the development of new efficient (bio)catalysts for the atmospheric carbon dioxide utilization. The ultimate goal is to use the abundant and economic carbon dioxide to produce energy and chemical feedstocks, while reducing an environmental pollutant. Certainly, understanding the chemistry used by nature to functionalize carbon dioxide should be valuable for this objective.

■ ASSOCIATED CONTENT

Supporting Information

The Supporting Information is available free of charge on the ACS Publications website at DOI: 10.1021/jacs.6b03941.

Figures S1–S5 and rate equations S1–S3. Detailed description of the kinetic model for the FDH-catalyzed formate oxidation and carbon dioxide reduction (Figure 4) and of the sulfur shift mechanism. Discussion of the EPR spectroscopic studies supporting the hydride transfer mechanism and of studies related with the selenocysteine dissociation from the molybdenum center and the direct formate binding to molybdenum. Discussion of possible mechanisms for the FDH reductive activation. (PDF)

■ AUTHOR INFORMATION

Corresponding Authors

*luisa.maia@fct.unl.pt

*jose.moura@fct.unl.pt

Notes

The authors declare no competing financial interest.

■ ACKNOWLEDGMENTS

This work was supported by the Unidade de Ciências Biomoleculares Aplicadas-UCIBIO, which is financed by national funds from FCT/MEC (UID/Multi/04378/2013) and cofinanced by the ERDF under the PT2020 Partnership Agreement (POCI-01-0145-FEDER-007728). LBM thanks Fundação para a Ciência e a Tecnologia, MEC, for a fellowship grant (SFRH/BPD/111404/2015, which is financed by national funds and cofinanced by FSE).

■ REFERENCES

(1) Appel, A. M.; Bercaw, J. E.; Bocarsly, A. B.; Dobbek, H.; DuBois, D. L.; Dupuis, M.; Ferry, J. G.; Fujita, E.; Hille, R.; Kenis, P. J.; Kerfeld, C. A.; Morris, R. H.; Peden, C. H.; Portis, A. R.; Ragsdale, S. W.; Rauchfuss, T. B.; Reek, J. N.; Seefeldt, L. C.; Thauer, R. K.; Waldrop, G. L. *Chem. Rev.* **2013**, *113*, 6621–6658.
(2) (a) Doney, S. C.; Fabry, V. J.; Feely, R. A.; Kleypas, J. A. *Annu. Rev. Mar. Sci.* **2009**, *1*, 169–192. (b) Friedlingstein, P.; Andrew, R. M.; Rogelj, J.; Peters, G. P.; Canadell, J. G.; Knutti, R.; Luderer, G.;

Raupach, M. R.; Schaeffer, M.; van Vuuren, D. P.; Le Quéré, C. *Nat. Geosci.* **2014**, *7*, 709–715.

(3) (a) D'Alessandro, D. M.; Smit, B.; Long, J. R. *Angew. Chem., Int. Ed.* **2010**, *49*, 6058–6082. (b) Langanke, J.; Wolf, A.; Hofmann, J.; Bohm, K.; Subhani, M. A.; Muller, T. E.; Leitner, W.; Gurtler, C. *Green Chem.* **2014**, *16*, 1865–1870. (c) Saeidi, S.; Amin, N. A. S.; Rahimpour, M. R. *J. CO₂ Util.* **2014**, *5*, 66–81. (d) Alissandratos, A.; Easton, C. J. *Beilstein J. Org. Chem.* **2015**, *11*, 2370–2387.

(4) (a) Glueck, S. M.; Gumus, S.; Fabian, W. M. F.; Faber, K. *Chem. Soc. Rev.* **2009**, *39*, 313–328. (b) Berg, I. A.; Kockelkorn, D.; Ramos-Vera, W. H.; Say, R. F.; Zarzycki, J.; Hugler, M.; Alber, B. E.; Fuchs, G. *Nat. Rev. Microbiol.* **2010**, *8*, 447–460. (c) Berg, I. A. *Appl. Environ. Microbiol.* **2011**, *77*, 1925–1936. (d) Fuchs, G. *Annu. Rev. Microbiol.* **2011**, *65*, 631–658. (e) Hugler, M.; Sievert, S. M. *Annu. Rev. Mar. Sci.* **2011**, *3*, 261–289. (f) Li, H.; Liao, J. C. *Energy Environ. Sci.* **2013**, *6*, 2892–2899.

(5) (a) Saveant, J.-M. *Chem. Rev.* **2008**, *108*, 2348–2378. (b) Benson, E. E.; Kubiak, C. P.; Sathrum, A. J.; Smieja, J. M. *Chem. Soc. Rev.* **2009**, *38*, 89–99. (c) Federsel, C.; Jackstell, R.; Beller, M. *Angew. Chem., Int. Ed.* **2010**, *49*, 6254–6257. (d) Kumar, B.; Llorente, M.; Froehlich, J.; Dang, T.; Sathrum, A.; Kubiak, C. P. *Annu. Rev. Phys. Chem.* **2012**, *63*, 541–569. (e) Costentin, C.; Robert, M.; Saveant, J.-M. *Chem. Soc. Rev.* **2013**, *42*, 2423–2436. (f) Ola, O.; Mercedes Maroto-Valer, M.; Mackintosh, S. *Energy Procedia* **2013**, *37*, 6704–6709. (g) Mondal, B.; Song, J.; Neese, F.; Ye, S. *Curr. Opin. Chem. Biol.* **2015**, *25*, 103–109.

(6) (a) Grimaldi, S.; Schoepp-Cothenet, B.; Ceccaldi, P.; Guigliarelli, B.; Magalon, A. *Biochim. Biophys. Acta, Bioenerg.* **2013**, *1827*, 1048–1085. (b) Hartmann, T.; Schwanhold, N.; Leimkühler, S. *Biochim. Biophys. Acta, Proteins Proteomics* **2014**, *1854*, 1090–1100. (c) Hille, R.; Hall, J.; Basu, P. *Chem. Rev.* **2014**, *114*, 3963–4038. (d) Maia, L. B.; Moura, J. J. G.; Moura, I. *JBIC, J. Biol. Inorg. Chem.* **2015**, *20*, 287–309.

(7) (a) Kato, N. *Methods Enzymol.* **1990**, *188*, 459–462. (b) Vinals, C.; Depiereux, E.; Feytmans, E. *Biochem. Biophys. Res. Commun.* **1993**, *192*, 182–188. (c) Popov, V. O.; Lamzin, V. S. *Biochem. J.* **1994**, *301*, 625–643. (d) Filippova, E. V.; Polyakov, K. M.; Tikhonova, T. V.; Stekhanova, T. N.; Boeeko, K. M.; Popov, V. O. *Crystallogr. Rep.* **2005**, *50*, 857–861. (e) Shabalina, I. G.; Polyakov, K. M.; Tishkov, V. I.; Popov, V. O. *Acta Nat.* **2009**, *1*, 89–93. (f) Alekseeva, A. A.; Savin, S.; Tishkov, V. I. *Acta Nat.* **2011**, *3*, 38–54.

(8) (a) Bursakov, S.; Liu, M.-Y.; Payne, W. J.; LeGall, J.; Moura, I.; Moura, J. J. G. *Anaerobe* **1995**, *1*, 55–60. (b) Sebban, C.; Blanchard, L.; Bruschi, M.; Guerlesquin, F. *FEMS Microbiol. Lett.* **1995**, *133*, 143–149. (c) Costa, C.; Teixeira, M.; LeGall, J.; Moura, J. J. G.; Moura, I. *JBIC, J. Biol. Inorg. Chem.* **1997**, *2*, 198–208. (d) Almendra, M. J.; Brondino, C. D.; Gavel, O.; Pereira, A. S.; Tavares, P.; Bursakov, S.; Duarte, R.; Caldeira, J.; Moura, J. J.; Moura, I. *Biochemistry* **1999**, *38*, 16366–16372. (e) Raaijmakers, H.; Teixeira, S.; Dias, J. M.; Almendra, M. J.; Brondino, C. D.; Moura, I.; Moura, J. J.; Romão, M. J. *JBIC, J. Biol. Inorg. Chem.* **2001**, *6*, 398–404. (f) Raaijmakers, H.; Macieira, S.; Dias, J. M.; Teixeira, S.; Bursakov, S.; Huber, R.; Moura, J. J.; Moura, I.; Romão, M. J. *Structure* **2002**, *10*, 1261–1272. (g) Brondino, C. D.; Passaggi, M. C. G.; Caldeira, J.; Almendra, M. J.; Feio, M. J.; Moura, J. J. G.; Moura, I. *JBIC, J. Biol. Inorg. Chem.* **2004**, *9*, 145–151. (h) Heidelberg, J. F.; Seshadri, R.; Haveman, S. A.; Hemme, C. L.; Paulsen, I. T.; Kolonay, J. F.; Eisen, J. A.; Ward, N.; Methe, B.; Brinkac, L. M.; Daugherty, S. C.; Deboy, R. T.; Dodson, R. J.; Durkin, A. S.; Madupu, R.; Nelson, W. C.; Sullivan, S. A.; Fouts, D.; Haft, D. H.; Selengut, J.; Peterson, J. D.; Davidsen, T. M.; Zafar, N.; Zhou, L.; Radune, D.; Dimitrov, G.; Hance, M.; Tran, K.; Khouri, H.; Gill, J.; Utterback, T. R.; Feldblyum, T. V.; Wall, J. D.; Voordouw, G.; Fraser, C. M. *Nat. Biotechnol.* **2004**, *22*, 554–559. (i) Rivas, M.; Gonzalez, P.; Brondino, C. D.; Moura, J. J. G.; Moura, I. *J. Inorg. Biochem.* **2007**, *101*, 1617–1622. (j) Mota, C. S.; Valette, O.; Gonzalez, P. J.; Brondino, C. D.; Moura, J. J. G.; Moura, I.; Dolla, A.; Rivas, M. G. *J. Bacteriol.* **2011**, *193*, 2917–2923. (k) Silva, S. M.; Pimentel, C.; Valente, F. M. A.; Rodrigues-Pousada, C.; Pereira, I. A. C. *J. Bacteriol.* **2011**, *193*, 2909–2917.

- (9) (a) Hille, R. *Chem. Rev.* **1996**, *96*, 2757–2816. (b) Maia, L.; Moura, I.; Moura, J. J. G. Molybdenum and Tungsten-Containing Enzymes: An Overview. In *Molybdenum and Tungsten Enzymes: Biochemistry - RSC Metallobiology Series No. 5*; Hille, R.; Schulzke, C.; Kirk, M., Eds.; The Royal Society of Chemistry, 2016.
- (10) Boyington, J. C.; Gladyshev, V. N.; Khangulov, S. V.; Stadtman, T. C.; Sun, P. D. *Science* **1997**, *275*, 1305–1308.
- (11) Raaijmakers, H. C. A.; Romão, M. J. *JBIC, J. Biol. Inorg. Chem.* **2006**, *11*, 849–854.
- (12) Jormakka, M.; Tornroth, S.; Byrne, B.; Iwata, S. *Science* **2002**, *295*, 1863–1868.
- (13) Cornish-Bowden, A. *Fundamentals of Enzyme Kinetics*; Portland Press: London, 1995.
- (14) Bassegoda, A.; Madden, C.; Wakerley, D. W.; Reisner, E.; Hirst, J. *J. Am. Chem. Soc.* **2014**, *136*, 15473–15476.
- (15) Mota, C. S.; Rivas, M. G.; Brondino, C. D.; Moura, I.; Moura, J. J. G.; Gonzalez, P. G.; Cerqueira, N.M.F.S.A. *JBIC, J. Biol. Inorg. Chem.* **2011**, *16*, 1255–1268.
- (16) The *as purified* FDH samples are most likely composed by a mixture of slightly different inactive forms (F_0' , F_0'' , F_0''' , ...), which would react with formate at different rates (k_5' , k_5'' , k_5''' , ... (Figure 4)). Nevertheless, the model included only one inactive form (F) and one active form (E) to avoid unnecessary complications that would not provide any extra useful information (and k_5 , k_{-5} , k_7 and k_{-7} can be thought as global rate constants).
- (17) Although Mota et al.¹⁵ had already proposed that FDH exists in two forms, one active and another inactive, this is the first demonstration that the long initial lag phases, with half-times of several minutes, can in fact be due to an inactive form of FDH, as long as its conversion into the active form is considerably slower than the other catalytic steps.
- (18) (a) Ruschig, W.; Muller, U.; Willnow, P.; Hopner, T. *Eur. J. Biochem.* **1976**, *70*, 325–330. (b) Muller, U.; Willnow, P.; Ruschig, U.; Hopner, T. *Eur. J. Biochem.* **1978**, *83*, 485–498. (c) Yamamoto, I.; Saikit, T.; Liu, S.-M.; Ljungdahl, L. *J. Biol. Chem.* **1983**, *258*, 1826–1832. (d) de Bok, F. A. M.; Hagedoorn, P. L.; Silva, P. J.; Hagen, W.; Schiltz, E.; Fritsche, K.; Stams, A. J. M. *Eur. J. Biochem.* **2003**, *270*, 2476–2485. (e) Ragsdale, S. W.; Pierce, E. *Biochim. Biophys. Acta, Proteins Proteomics* **2008**, *1784*, 1873–1898. (f) Reda, T.; Plugge, C. M.; Abram, N. J.; Hirst, J. *Proc. Natl. Acad. Sci. U. S. A.* **2008**, *105*, 10654–10658. (g) Bruant, G.; Levesque, M.-J.; Peter, C.; Guiot, S. R.; Masson, L. *PLoS One* **2010**, *5*, e13033. (h) Armstrong, F. A.; Hirst, J. *Proc. Natl. Acad. Sci. U. S. A.* **2011**, *108*, 14049–14054. (i) Alissandratos, A.; Kim, H.-K.; Matthews, H.; Hennessy, J. E.; Philbrook, A.; Easton, C. J. *Appl. Environ. Microbiol.* **2013**, *79*, 741–744. (j) Hartmann, T.; Leimkuhler, S. *FEBS J.* **2013**, *280*, 6083–6096. (k) Schuchmann, K.; Müller, V. *Science* **2013**, *342*, 1382–1385. (l) [154] Martins, M.; Mourato, C.; Pereira, I. A. C. *Environ. Sci. Technol.* **2015**, *49*, 14655–14662.
- (19) (a) Jacques, J. G. J.; Fourmond, V.; Arnoux, P.; Sabaty, M.; Etienne, E.; Grosse, S.; Biaso, F.; Bertrand, P.; Pignol, D.; Léger, C.; Guigliarelli, B.; Burlat, B. *Biochim. Biophys. Acta, Bioenerg.* **2014**, *1837*, 277–286. (b) Garton, S. D.; Hilton, J.; Oku, H.; Crouse, B. R.; Rajagopalan, K. V.; Johnson, M. K. *J. Am. Chem. Soc.* **1997**, *119*, 12906–12916.
- (20) (a) Fourmond, V.; Burlat, B.; Dementin, S.; Arnoux, P.; Sabaty, M.; Boiry, S.; Guigliarelli, B.; Bertrand, P.; Pignol, D.; Léger, C. *J. Phys. Chem. B* **2008**, *112*, 15478–15486. (b) Ceccaldi, P.; Rendon, J.; Léger, C.; Toci, R.; Guigliarelli, B.; Magalon, A.; Grimaldi, S.; Fourmond, V. *Biochim. Biophys. Acta, Bioenerg.* **2015**, *1847*, 1055–1063. (c) Field, S. J.; Thornton, N. P.; Anderson, L. J.; Gates, A. J.; Reilly, A.; Jepson, B. J. N.; Richardson, D. J.; George, S. J.; Cheesman, M. R.; Butt, J. N. *Dalton Trans* **2005**, 3580–3586. (d) George, G.; Hilton, J.; Temple, C.; Prince, R.; Rajagopalan, K. *J. Am. Chem. Soc.* **1999**, *121*, 1256–1266.
- (21) (a) Massey, V.; Edmondson, D. *J. Biol. Chem.* **1970**, *245*, 6595–6598. (b) Olson, J. S.; Ballou, D. P.; Palmer, G.; Massey, V. *J. Biol. Chem.* **1974**, *249*, 4363–4382. (c) Coughlan, M. P.; Johnson, J. L.; Rajagopalan, K. V. *J. Biol. Chem.* **1980**, *255*, 2694–2699.
- (22) (a) Barber, M. J.; May, H. D.; Ferry, J. G. *Biochemistry* **1986**, *25*, 8150–8155. (b) Friedebold, J.; Bowien, B. *J. Bacteriol.* **1993**, *175*, 4719–4728. (c) Thomé, R.; Gust, A.; Toci, R.; Mendel, R.; Bittner, F.; Magalon, A.; Walburger, A. *J. Biol. Chem.* **2012**, *287*, 4671–4678.
- (23) (a) Edmondson, D. E.; Ballou, D.; Vanheuvelen, A.; Palmer, G.; Massey, V. *J. Biol. Chem.* **1973**, *248*, 6135–6144. (b) Xia, M.; Dempski, R.; Hille, R. *J. Biol. Chem.* **1999**, *274*, 3323–3330.
- (24) (a) Boll, M. *Biochim. Biophys. Acta, Bioenerg.* **2005**, *1707*, 34–50. (b) Johannes, J.; Unciuleac, M.; Friedrich, T.; Warkentin, E.; Ermler, U.; Boll, M. *Biochemistry* **2008**, *47*, 4964–4972.
- (25) Thauer, R. K.; Kaufer, B.; Fuchs, G. *Eur. J. Biochem.* **1975**, *55*, 111–117.
- (26) Khangulov, S. V.; Gladyshev, V. N.; Dismukes, G. C.; Stadtman, T. C. *Biochemistry* **1998**, *37*, 3518–3528.
- (27) All known FDHs harbor an active site with one molybdenum or one tungsten atom coordinated, in the oxidized state, by four sulfur atoms from two pyranopterin molecules, one terminal sulfo group (Mo=S) plus a selenocysteine (Mo-Se(Cys)) or cysteine residue (Mo-S(Cys)). Although all known tridimensional structures are from enzymes harboring an active site selenocysteine (Figure S1), it is known since the 1980s that there are FDHs that do not have a selenocysteine residue, such as the enzymes from *Methanobacterium formicicum*^{28a,b} or *Ralstonia eutropha*,^{28c,d} *Methylobacterium extorquens*^{28e} or *Rhodobacter capsulatus*.^{18j}
- (28) (a) Schauer, N. I.; Ferry, J. F. *J. Bacteriol.* **1982**, *150*, 1–7. (b) Johnson, J. L.; Bastian, N. R.; Schauer, N. L.; Ferry, J. G.; Rajagopalan, K. V. *FEMS Microbiol. Lett.* **1991**, *77*, 213–216. (c) Friedebold, J.; Bowien, B. *J. Bacteriol.* **1993**, *175*, 4719–4728. (d) Oh, J. I.; Bowien, B. *J. Biol. Chem.* **1998**, *273*, 26349–26360. (e) Laukel, M.; Chistoserdova, L.; Lidstrom, M. E.; Vorholt, J. A. *Eur. J. Biochem.* **2003**, *270*, 325–333.
- (29) (a) Leopoldini, M.; Chiodo, S. G.; Toscano, M.; Russo, N. *Chem. - Eur. J.* **2008**, *14*, 8674–8681. (b) Tiberti, M.; Papaleo, E.; Russo, N.; Gioia, L.; Zampella, G. *Inorg. Chem.* **2012**, *51*, 8331–8339.
- (30) Cerqueira, N.M.F.S.A.; Fernandes, P. A.; Gonzalez, P. J.; Moura, J. J. G.; Ramos, M. J. *Inorg. Chem.* **2013**, *52*, 10766–10772.
- (31) Schrapers, P.; Hartmann, T.; Kositzki, R.; Dau, H.; Reschke, S.; Schulzke, C.; Leimkuhler, S.; Haumann, M. *Inorg. Chem.* **2015**, *54*, 3260–3271.
- (32) Niks, D.; Duvvuru, J.; Escalona, M.; Hille, R. *J. Biol. Chem.* **2016**, *291*, 1162–1174.
- (33) (a) Stiefel, E. I. *Proc. Natl. Acad. Sci. U. S. A.* **1973**, *70*, 988–992. (b) Stiefel, E. I. *Prog. Inorg. Chem.* **1977**, *21*, 1–223. (c) Rajapakshe, A.; Snyder, R. A.; Astashkin, A. V.; Bernardson, P.; Evans, D. J.; Young, C. G.; Evans, D. H.; Enemark, J. H. *Inorg. Chim. Acta* **2009**, *362*, 4603–4608.
- (34) It is not chemically reasonable to have a selenium/sulfur atom with three bonds and a positive charge (one bond to the amino acid side chain, plus one bond to the metal and another bond to the hydrogen). Theoretical calculations of the activation energy for the C–H bond cleavage also showed that the proton abstraction by a bound selenocysteine is highly unfavorable (36 kcal/mol).^{29a}
- (35) (a) Tanaka, R.; Yamashita, M.; Nozaki, K. *J. Am. Chem. Soc.* **2009**, *131*, 14168–14169. (b) Ziebart, C.; Federsel, C.; Anbarasan, P.; Jackstell, R.; Baumann, W.; Spannenberg, A.; Beller, M. *J. Am. Chem. Soc.* **2012**, *134*, 20701–20704. (c) Jeletic, M. S.; Mock, M. T.; Appel, A. M.; Linehan, J. C. *J. Am. Chem. Soc.* **2013**, *135*, 11533–11536. (d) Wang, W.-H.; Muckerman, J. T.; Fujita, E.; Himeda, Y. *ACS Catal.* **2013**, *3*, 856–860. (e) Filonenko, G. A.; Hensen, E. J. M.; Pidko, E. A. *Catal. Sci. Technol.* **2014**, *4*, 3474–3485.
- (36) Mota, C. S. PhD Thesis, Faculdade de Ciências e Tecnologia, Universidade Nova de Lisboa, Portugal, 2011; <http://hdl.handle.net/10362/6688>.
- (37) Weinert, T.; Huwiler, S. G.; Kung, J. W.; Weidenweber, S.; Hellwig, P.; Stärk, H.-J.; Biskup, T.; Weber, S.; Cotelesage, J. J. H.; George, G. N.; Ermler, U.; Boll, M. *Nat. Chem. Biol.* **2015**, *11*, 586–591.
- (38) Curiously, XO, which holds a penta-coordinated molybdenum center, is inhibited by formaldehyde, and it has been suggested that

during the hydroxylation of formaldehyde, the formate moiety formed binds tightly in a bidentate mode to the XO molybdenum, thus blocking the molybdenum center and inhibiting the enzyme.³⁹ This inhibition can be regarded as an indirect evidence that formate can not be handled by a penta-coordinated molybdenum center.

(39) (a) Pick, F. M.; McGartoll, M. A.; Bray, R. C. *Eur. J. Biochem.* **1971**, *18*, 65–72. (b) Howes, B. D.; Pinhal, N. M.; Turner, N. A.; Bray, R. C.; Anger, G.; Ehrenberg, A.; Raynor, J. B.; Lowe, D. J. *Biochemistry* **1990**, *29*, 6120–6127.

(40) Lothrop, A. P.; Snider, G. W.; Flemer, S., Jr.; Ruggles, E. L.; Davidson, R. S.; Lamb, A. L.; Hondal, R. J. *Biochemistry* **2014**, *53*, 664.

(41) Heider, J.; Bock, A. *Adv. Microb. Physiol.* **1993**, *35*, 71–109.

(42) Of note, there are also NAD-dependent Mo-FDHs and W-FDHs⁶ and these enzymes should not be confused with the NAD-dependent metal-independent FDHs. In the metal-independent FDHs, the reducing equivalents, obtained from formate oxidation or necessary to carbon dioxide reduction, are directly transferred to NAD⁺ or from NADH (respectively). In the metal-dependent FDHs, the reducing equivalents are first transferred to the other(s) redox-active center(s) of the enzyme and, finally, to the oxidizing substrate, which, in the case of NAD-dependent Mo-FDHs and W-FDHs, is also a NAD⁺ or NADH molecule.